energies

MDPI

Article

Gear Ratio Optimization along with a Novel Gearshift Scheduling Strategy for a Two-Speed Transmission System in Electric Vehicle

Md Ragib Ahssan [1,*], Mehran Ektesabi [2] and Saman Gorji [3]

[1] Department of Mechanical Engineering and Product Design Engineering, Swinburne University of Technology, Melbourne 3122, Australia
[2] Department of Telecommunications, Electrical, Robotics and Biomedical Engineering, Swinburne University of Technology, Melbourne 3122, Australia; mektesabi@swin.edu.au
[3] Institute for Future Environments, Queensland University of Technology, Brisbane 4001, Australia; saman.asgharigorji@qut.edu.au
* Correspondence: mahssan@swin.edu.au; Tel.: +61-3-9214-4965

Received: 24 August 2020; Accepted: 25 September 2020; Published: 28 September 2020

Abstract: A novel gearshift scheduling strategy has been framed for a two-speed transmission system in electric vehicles that can save energy during hilly driving and frequently changing driving conditions through efficient electric motor operation. Unlike the traditional approach, the proposed gearshift strategy is based on the preferred vehicle speed range, vehicle acceleration, and road grade to ensure desired vehicle performances with minimum energy consumption. Meanwhile, the vehicle speed range is chosen around the electric motor rated speed, and two gearshift schedules in relation to vehicle acceleration and road grade are developed based on the motor torque generating capacity and efficiency. Appropriate gear is selected through a combined assessment of the required vehicle speed, acceleration, and road grade information. A guideline is developed and explained for the primary gearshift schedule. Next, the gear ratios and gearshift schedules are optimized combinedly in a Simulink environment using the gradient descent method and pattern search method on three driving cycles separately. Depending on the driving scenarios, around 4% to 7.5% energy saving has been experienced through optimization, while the gear ratios and gearshift schedule in relation to the road grade are found to be major contributors to the vehicle economic driving compared to that with the gearshift schedule for vehicle acceleration.

Keywords: electric vehicle; multi-speed transmission; gearshift scheduling strategy; gear ratio optimization; vehicle performances

1. Introduction

Incorporating the multi-speed transmission system in electric vehicles (EVs) could be a solution to achieve better drivetrain efficiency. In the review paper by Ahssan et al. [1], it has been shown how the multi-speed transmission system outperforms the single-speed transmission system in EVs. However, the multi-gear system introduces additional complexities such as the selection of optimal gear ratios, appropriate gearshift schedule and shifting control, torque interruption during gear shifting, increased mass, and transmission loss. In this study, an appropriate gearshift schedule strategy, and then, optimization of both gear ratios and the gearshift schedule will be investigated.

A higher value of gear ratio contributes to achieving higher gradeability and faster acceleration, while a lower value of gear ratio determines the maximum vehicle speed limit and reduces energy consumption [2,3]. The gearshift schedule dictates the initiation of gear change i.e., either upshift or downshift depending on the demand of vehicle performances. Vehicle driving economy or dynamic

performances can be prioritized by developing an appropriate shift schedule [4]. Therefore, identifying parameters that might be involved to develop the shifting schedule is important as well as complex.

In many studies concerning the optimization of gear ratios and shift scheduling, the gearshift is initiated based on two common parameters i.e., throttle position or torque demand and vehicle speed, as shown in Table 1, to reduce the computational load of the optimization process. Electric motor or traction motor efficiency at each instance of the vehicle speed and torque demand is considered to choose the gear with the highest motor efficiency [5]. Zhou et al. [6], and Morozov et al. [7] studied the impact of different gear ratios on EV performances with standard or fixed shift schedules. Morozov et al. [7] used motor speed as the gearshift parameter that may cause a shift hunting problem due to the motor speed fluctuation during the gear shifting phase. To make it comprehensive, Zhu et al. [8] and Zhou et al. [9] presented an auto-search method of optimizing the gear ratios and shift schedule simultaneously. According to this method, the gearshift schedule line is drawn by connecting the intersection points between the electric motor efficiency lines for two consecutive gears at several sets of throttle position and vehicle speed. Although the developed gearshift schedule has been applied in other studies conducted by Ruan et al. [10] and Ruan et al. [11], this technique is inherently complex. Moreover, although the motor efficiency and different vehicle driving conditions are considered, in practice, the traditional rule-based (i.e., throttle position and vehicle speed) gearshift schedule is a fixed gearshift schedule and may be effective for certain driving scenarios.

Table 1. Gear shift scheduling parameters considered in recent studies on the multi-gear transmission system in EVs.

EV Transmission Model	Gear Ratios	Shift Scheduling Parameters	Limitations of Shift Scheduling Strategy
4-Speed [10]	14.4/10.4/7.2/5.2	Throttle Position Vehicle speed	Suitable for flat road and may not be suitable for all driving cycles simultaneously. It is ensured that a certain velocity will be achieved at maximum road gradient. However, appropriate gear selection during changing road gradient cannot be addressed.
4-Speed [12]	27.72/14.92/9.7/4.74	Throttle Position Motor speed	
2-Speed [7]	5.9/3.11	Throttle Position Motor speed	
2-Speed [4]	10.63/5.12	Throttle opening Vehicle speed	
2-Speed [9]	9.39/4.83	Throttle angle Vehicle speed	
2-Speed [13]	11.47/4.64	Throttle angle Vehicle speed	
2-Speed [14]	9.8/3.56	Accelerator opening Vehicle speed	
2-Speed [2]	-	Driver demand Vehicle speed	
2-Speed [15]	-	Driver demand Vehicle speed	

In the above-mentioned research papers, maximum gradeability is set as one of the dynamic performance targets, but energy consumption on a route with frequently varied altitude has not been studied. Moreover, standard drive cycles i.e., New European Drive Cycle (NEDC), Urban Dynamometer Driving Schedule (UDDS), etc. are based on the flat road [16]. Recently, Han et al. [17] presented a systematic framework to optimize the gear numbers, gear ratios, and gearshift schedule in the transmission system for EVs considering several driving conditions. In another study, Li et al. [18] conducted parameter optimization of both the electric motor and a two-speed transmission system in an EV. Both research groups used the road inclination to set the dynamic performance target and the upper limit of the gear ratios during the optimization process. However, road inclination is ignored in the driving cycles. A single gearshift schedule may not be equally suitable or efficient for all drive cycles without compromising the vehicle performances. It is also difficult to come up with a single optimized gearshift schedule that would ensure efficient motor operation in all possible driving scenarios. The suggested gearshift schedule strategy will assess motor speed, vehicle acceleration and road grade to initiate the gearshift and will address the mentioned shortcomings. In the next section, typical models of major powertrain components in EV are briefly described along with a detailed explanation of shift schedule strategy for a two-speed transmission unit that can be further extended to a multi-speed transmission system in electric vehicle. In Section 3, a combined gear ratio and shift schedule optimization process is explained. The results are analyzed in the fourth section followed by conclusion in Section 5.

2. EV Powertrain

Major components of EV powertrain include a battery, an electric motor, and a transmission system. All the components are modeled within MATLAB/Simulink environment. In the following sub-sections, the functionality of the battery and electric motor blocks is briefly explained along with their specifications. The transmission unit is described in detail as the focus of this study. To evaluate the performances of the proposed gearshift schedule strategy for a two-speed transmission system in electric vehicles, the parameters of a large-size vehicle shown in Table 2 have been collected from a published research paper [6]. The inertial mass of the vehicle has been estimated as $m_{inertia} = 336.45$ kg based on the information of inertia of parts and associated formula provided in research papers by Lucente et al. [19] and Saini et al. [12], respectively.

Table 2. Vehicle parameter.

Vehicle Parameter	Symbol	Value	Unit
Vehicle Mass	m	1780	kg
Frontal Area	A	2.2	m^2
Wheel Radius	r_w	0.267	m
Final Drive Ratio	i_f	4.0	-
Wind Velocity	V_{wind}	0	Km/h
Drag Coefficient	C_d	0.28	-
Air Density	ρ	1.27	kg/m^3
Rolling Coefficient	μ	0.016	-
Gravity	g	9.81	m/s^2
Pi	π	3.14159	-
Road Incline	θ	0	deg
	$grd = (\theta \times \pi/180)$	0	rad

The vehicle model receives the information of the input drive cycle speed, road grade, and wind speed as inserted in the Simulink constant block and generates an output vehicle speed based on the following equation of motion i.e., Equation (1), where η_{PT} is the powertrain efficiency and GR_i is the gear ratios [13]. Here, GR_i is representing the product of actual gear ratios and the final drive ratio, i_f. Meanwhile, wind speed is assumed to be insignificant or zero; drive cycles and road grade information will be further explained later in this study.

$$\left.\begin{array}{r} \textit{Electric Motor Torque} = (\textit{Acceleration Force} + \textit{Resistance Force}) * \textit{Wheel Radius} \\ T_M = \frac{1}{\eta_{PT} GR_i} \times \left[(m + m_{inertia}) \times \frac{dV}{dt} + \left\{ m \times g \times (\mu \times \cos\theta + \sin\theta) + 0.5 \times C_d \times \rho \times A \times \left(\frac{V}{3.6}\right)^2 \right\} \right] \times r_w \end{array}\right\} \quad (1)$$

2.1. Battery

The battery unit stores the electric energy as presented in Table 3 and supplies it to the traction motor. However, the battery block is connected to the electric motor block as a backward-facing module in the EV model for simulation. This unit receives power demand P_M from the electric motor and adjusts it with its energy capacity over time.

Table 3. Battery energy capacity [8].

Battery Parameter	Symbol	Value	Unit
Voltage	V_{bat}	372	Volt
Capacity	Q_{max}	66	Ah
Energy	Em	24.55	kWh

When the battery state-of-charge, *SOC*, falls below a certain value i.e., 5%, it stops the simulation as an indication of a critical level of *SOC*. A single battery cell is modeled based on the lookup table data on cell voltage versus battery state-of-charge, *SOC*. Next, the battery output voltage is estimated according to the total number of battery cells considering both parallel and series arrangement.

$$SOC = \frac{Q_{current}}{Q_{max}} \times 100\% \tag{2}$$

$$Q_{current} = Q_{max} - \int_0^t \frac{I_{bat}}{3600 \times N_{cell\_p}} dt \tag{3}$$

$$I_{bat} = \frac{P_M}{V_{bat}} \tag{4}$$

$$V_{bat} = \left\{V_{OC} - (1/N_{cell\_p}) \times I_{bat} \times R_{int}\right\} \times N_{cell\_s} \tag{5}$$

$$V_{OC} = f(SOC) \tag{6}$$

$$R_{int} = f(SOC, temp) \tag{7}$$

Equations (2)–(5) explain how the battery state-of-charge, *SOC*, and battery voltage, V_{bat}, are estimated. Here, I_{bat} is the battery current, while N_{cell_s} and N_{cell_p} are the number of battery cells connected in series and parallel. The battery open-circuit voltage, V_{OC}, and battery internal resistance, R_{int}, are the function of battery state-of-charge, *SOC*, and the surrounding temperature, *temp*, as shown in Equations (6) and (7), and these are recalled from the look-up table data retained in the battery block in Simulink.

2.2. Electric Motor

A map-based motor model from the Simulink Powertrain Blockset toolbox is used for simulation. The motor model is integrated with two lookup tables in Simulink. One lookup table provides maximum torque vs. speed data while the other holds motor efficiency data at numerous torque–speed combinations as referred in Equations (8) and (9). Different types of electric motors, i.e., a permanent magnet motor, switched-reluctance motor, induction motor, etc. can be chosen for EVs depending on their robustness and availability. Characteristics of these types of electric motors are discussed in detail in the literature [20–23]. Interested readers are referred to [24–26] for in-depth knowledge on the control and modeling of electric motor for EVs. While some research can be found with more than one electric motor as the propulsion device in EVs [27,28], a single electric motor is considered in this study as the propulsion device. Table 4 shows the motor capacity that is collected from a published article by Zhu et al. [8]. The motor power, P_M, comprises the required motor output power at the input side of the transmission system, i.e., mechanical power, P_{Mech}, and loss of power, P_{Loss}, to generate that required mechanical power at any combination of the required electric motor output torque, T_M, and speed, n_M, as shown in Equation (10). Being a secondary module in the EV model, the battery block shows the drop in the battery state-of-charge, *SOC*, over time based on the motor power, P_M.

$$T_{M_{max}} = f(n_M), \tag{8}$$

$$\eta_M = f(T_M, n_M), \tag{9}$$

$$P_M = (P_{Mech} + P_{Loss}) = \{T_M \times 2 \times \pi \times n_M/60 + (1 - \eta_M) T_M \times 2 \times \pi \times n_M/60\}. \tag{10}$$

Efficiency data are extracted from the available motor efficiency map shown in Figure 1. During the simulation, the motor efficiency value at any torque–speed combination is determined through linear interpolation/extrapolation. The electric motor unit receives an acceleration command from the driver module, generates the required torque based on lookup table data, and transfers it to the transmission unit. A fully pressed acceleration pedal is linked to the maximum motor output torque generation at

any speed, while any fraction of the acceleration pedal is decoded as how much motor output torque is needed to be scaled down from its maximum limit.

Table 4. Traction motor parameter [8].

Traction Motor Parameter	Symbol	Value	Unit
Rated Power	P_m	40	kW
Rated Torque	T_m	127	Nm
Base Speed	n_b	3000	rpm
Maximum Power	$P_{M_{max}}$	80	kW
Maximum Torque	$T_{M_{max}}$	255	Nm
Maximum Speed	n_{max}	9000	rpm

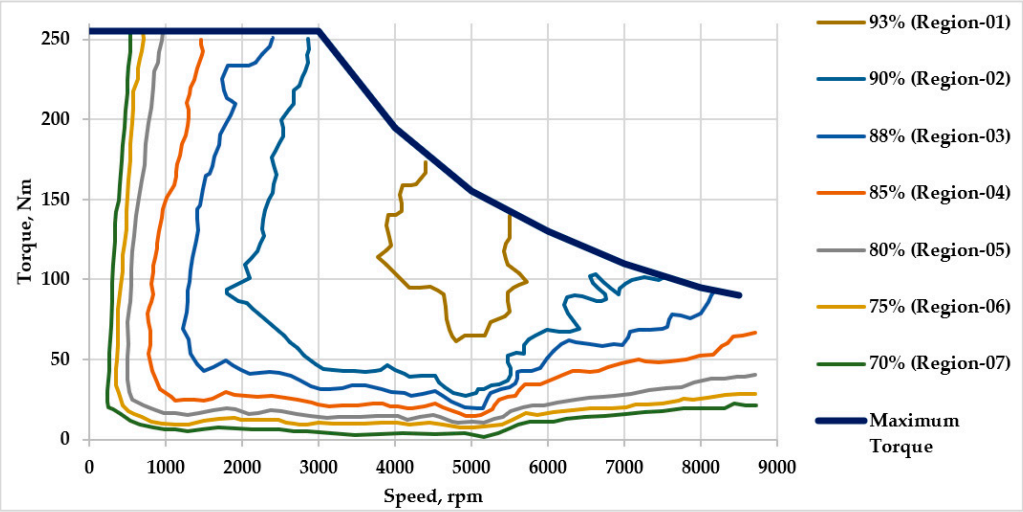

Figure 1. Maximum torque capacity and efficiency maps of the motor [8].

2.3. Transmission

In conventional internal combustion engine (ICE) vehicles, higher number of gears are used in the transmission system to reduce fuel consumption [29]. However, that is not the case with EV because of the torque–speed characteristics of the electric motor i.e., high torque at the lower speed region and a constant power region throughout the extended speed range [21], and fewer gears could serve the purpose of achieving the required vehicle performances [13]. A two-speed automatic manual/mechanical transmission (AMT) system is considered for the EV model in this study. For an EV powertrain, several types of multi-speed transmission system are available to choose such as automatic transmission (AT) [30,31], continuous variable transmission (CVT), dual-clutch transmission (DCT) [32,33], inverse automatic mechanical transmission (IAMT) [4,34], uninterrupted mechanical transmission (UMT) [35], automatic mechanical transmission (AMT), etc. Each type of transmission system has its own benefits or limitations. Chai et al. [36] and Kim et al. [37] made enough reasonings in favor of using AMT in EVs. Some of those are features of ATs with higher-energy economy, higher controllability, converting existing manual transmission (MT) into AMT causing lower development cost, etc.

As shown in Figure 2, an AMT can generally be formed by adding an actuator (i.e., hydraulic actuator or small electric motor) and sensors to the traditional MT and by removing the existing clutch arrangement. The gearshift is conducted through an actuator according to the command from the transmission control unit (TCU). As a result of the high torque-speed controllability of the traction motor, it is possible to adjust the torque and speed between the rotor and input shaft of transmission during gear disengagement and engagement in the gearshift process to minimize the torque interruption at the vehicle wheels. Based on these criteria, AMT is considered as a reasonable choice for this study.

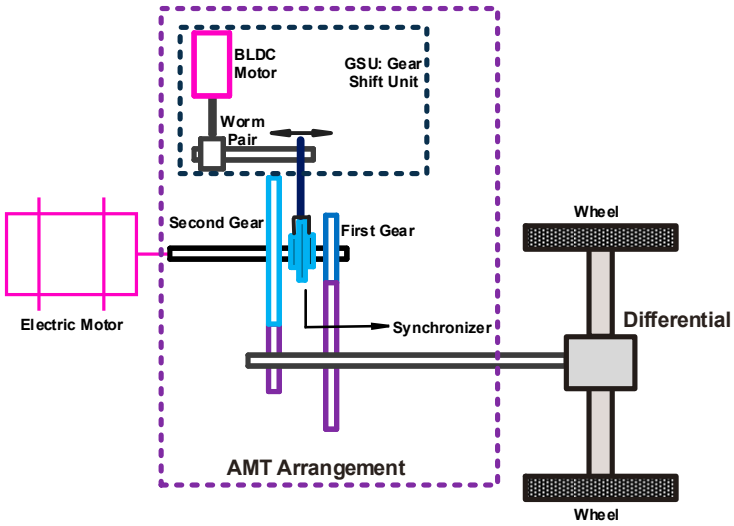

Figure 2. A typical automatic manual/mechanical transmission (AMT) layout within an electric vehicle (EV) powertrain.

The role of the transmission system is to ensure enough wheel torque to run the vehicle at maximum road grade and at desired maximum speed and to achieve faster acceleration with minimum energy consumption. Based on recent literature on the multi-gear transmission system in an EV, Table 5 demonstrates the targets of the vehicle dynamic performances that have been set to evaluate the performances of the proposed gearshift scheduling strategy for two-speed AMT in an EV. A comprehensive discussion can be found in [10,38], where the efficiency of a two-speed DCT may vary from 86% to 95% depending on the gear number and other factors i.e., viscous loss, wet clutch loss, synchronizer mechanism, differential, etc. However, in this study, the efficiency of the two-speed AMT system is considered as 90% on gear 1 and 95% on gear 2. In the following sub-sections, the novel gearshift strategy is explained about how this would meet up the target vehicle performances as well as save energy consumption at different driving conditions.

Table 5. Targets for vehicle dynamic performances.

Vehicle Performances		Symbol	Target	Unit
Maximum Gradeability		θ_{max}	23	deg
		grd_{max}	0.401587302	rad
Velocity at Maximum Grade		V_grd_{max}	15	km/h
Maximum Vehicle Velocity		V_{max}	150	km/h
Acceleration Time	0–60 km/h	t_{0-60}	5.5	Sec
	60–80 km/h	t_{60-80}	3.5	
	0–100 km/h	t_{0-100}	13	

3. Proposed Shift Scheduling Strategy

A three-parameter-based gearshift strategy has been formulated to choose appropriate gear at various driving conditions. These parameters are vehicle speed, road grade, and vehicle acceleration, which are estimated in real time. Vehicle speed information can be directly available through the speedometer, while acceleration can be calculated by differentiating the current velocity. Although real-time road grade information is not common in most of the present production vehicle control systems [39], road grade estimation is becoming significant for advanced driver assistance system (ADAS), fuel economy, intelligent energy management strategy (EMS), and autonomous cars [40,41]. In the literature, several approaches for real-time road grade estimation can be found such as recursive least squares (RLS) using

vehicle longitudinal dynamic models [42,43], adaptive extended Kalman filter (AEKF) [44], parallel mass and grade (PNG) estimation [45], grade estimation through orientation filter from inertial measurement unit (IMU) data [40], etc. Within the scope of this study, it is assumed that any approach of road grade estimation would meet up the requirement for this study, and road grade information would be available as a feature of ADAS. The upper and lower bound of each parameter are set for upshift and downshift, respectively. Then, a set of shift logic initiates the change of gear considering the combined assessment of all three parameters.

3.1. Gearshift Schedule Parameter–Vehicle Speed

The vehicle speed range is set based on the rated motor speed, n_b i.e., 3000 rpm, as shown in Table 4, because it is known that the motor runs most efficiently at its rated speed. For the preferred motor speed range, there will be two sets of vehicle speed range due to considering two gears. Motor speed is not considered directly in decision making because of the sudden fluctuation of motor speed during gearshift to avoid the gear hunting problem. When the vehicle speed goes above the upshift speed of gear 1, then gear 2 will be allowed to select. Next, when the vehicle speed goes below the downshift speed of gear 2, then gear 1 will be the preferred choice.

3.2. Gearshift Schedule Parameter–Road Grade and Vehicle Acceleration

Initially, two separate shifting maps are developed to meet up the torque demands at various road grades and accelerations. To generate the gearshift maps, the maximum and rated capacity of the electric motor i.e., torque, speed, power, and motor efficiency at each gear, as shown in Figures 1 and 3, as well as common driving scenarios, industrial practice, and knowledge are the considerations.

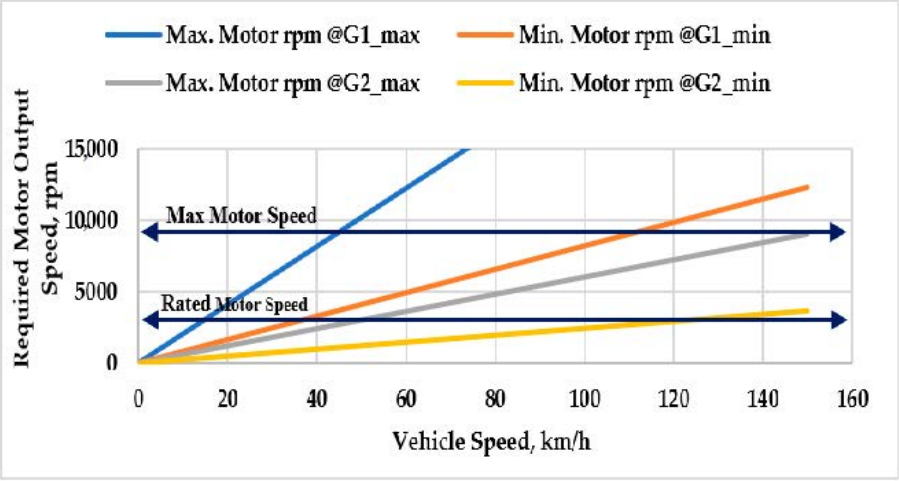

Figure 3. Required motor output speed against desired vehicle speed at the upper and lower bounds of gear 1 and gear 2.

An imaginary schedule line or a separation line as shown in Figure 4 is developed to identify the efficient operation area of the electric motor at each gear among the two consecutives. Several representative points are identified on both the road grade vs. vehicle speed and acceleration vs. vehicle speed graph. These points can be named as transition points between two consecutive gears. The gearshift schedule line is achieved by connecting those points in relation to road grade and vehicle acceleration. Then, to avoid the gear hunting problem, this schedule line will be split up into two lines by imposing a weighting factor. The line on the left side represents the downshift line, while the line on the right side stands for the upshift.

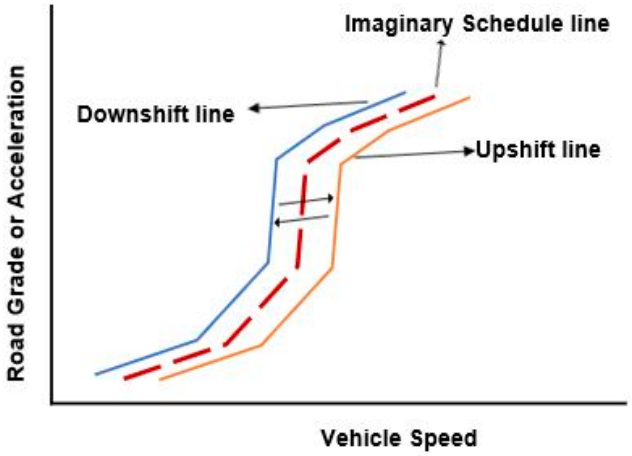

Figure 4. Imaginary schedule line or separation line for the gearshift.

The gearshift schedule achieved at this stage can be considered as the primary gearshift schedule to run the simulation of the EV model. Next, the primary shift schedule will be further optimized through an appropriate optimization process. A guideline is articulated here about how the primary gearshift schedule can be generated with less effort.

- Considering vehicle acceleration at different vehicle speed ranges and various road grades at different constant vehicle speeds, numerical analysis on the motor torque requirements has been conducted based on Equation (1). For any condition, there are three possible choices for a two-speed transmission system; i.e., the first is that only gear 1 can provide the required wheel torque at this vehicle speed, the second choice is only gear 2 can be the option, and the third is any gear can be chosen to supply the necessary torque and speed at the vehicle wheel. For the third scenario, the gear with the higher motor efficiency can be chosen to save energy consumption. Therefore, it is convenient to identify the three-speed regions such that each speed region can be associated with any of the above three choices as stated. At the low-speed region i.e., zero to approximately 20–25 km/h, gear 1 is an obvious option because of the high torque demand from the motor to meet up with the requirements at the initial vehicle acceleration or uphill driving scenario. Practically, gear 2 is not an option in this speed range, because the required motor output torque exceeds the maximum motor output torque limit in many cases or the motor operates at a very low efficiency region.
- Similarly, at a high-speed region i.e., 65–70 km/h or above, gear 1 cannot be selected, because the required motor speed goes over the maximum speed limit of the motor. Therefore, gear 2 can be set as the default selection in this speed range.
- Now, the gear selection problem can be narrowed down to the vehicle speed range between 20–25 km/h and 65–70 km/h where any gear could be a choice to meet up the requirements to run the vehicle. Here, the motor efficiency and rated motor capacity play the decision-making role for gear selection. Transition points for gear change are identified where the required motor output torque and speed at both gears are close to its rated capacity. Gear one is preferred at the vehicle speed below the speed corresponding to the transition points, and gear two is selected when the vehicle speed goes over the speed at the transition points. Next, the imaginary separation line can be achieved by connecting the transition points.
- An imaginary separation line needs to be split up into two lines i.e., upshift and downshift lines, to avoid frequent gearshift through applying an appropriate weighting factor. Zhang et al. [46] used a hysteresis strategy where the gearshift line is increased by 20% to set the upshift line and is decreased by 20% for the downshift line. Another common technique of implementing a weighting factor is to apply a penalty factor within the optimization algorithm to prevent the repeated gearshift [47,48]. Although these techniques are applied on throttle demand vs. vehicle

speed-based gearshift schedule and cannot be directly linked to the proposed schedule in relation to road grade and vehicle acceleration, these could be considered as a general guideline. In this study, the weighting factor is set manually considering mainly two factors [49], i.e., avoiding frequent gearshift to ensure rider comfort and kick-downshifting during high acceleration demand. Therefore, the weighting factor is not necessarily the same at all vehicle speeds. However, a buffer zone of 10–40% has been maintained between the downshift line and upshift line that will be further optimized through applying an appropriate optimization method in the later part of this paper.

- Following the above steps, primary gearshift schedules in relation to the vehicle acceleration and road grade have been shown in Figures 5 and 6, respectively.

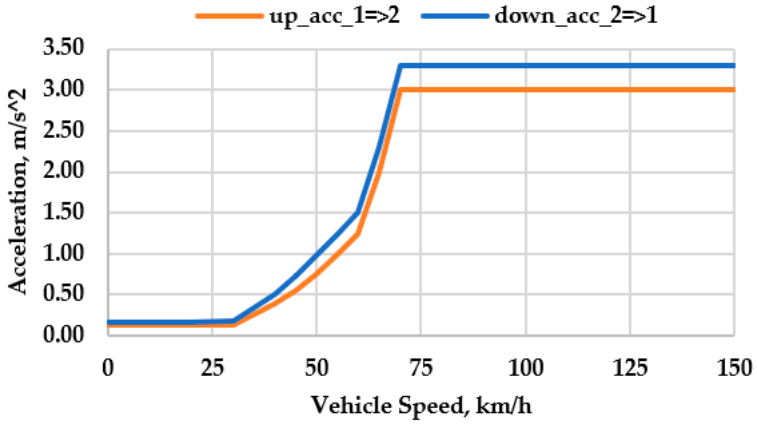

Figure 5. Gearshift schedule map based on the vehicle acceleration.

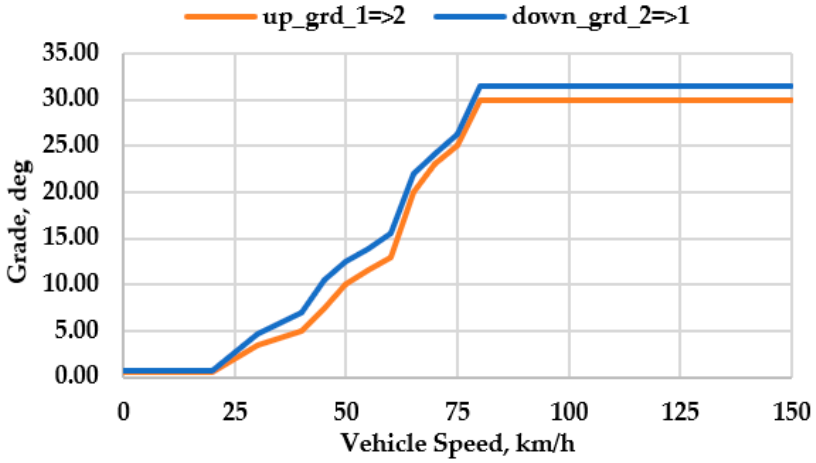

Figure 6. Gearshift schedule map based on the road grade.

3.3. Gearshift Control

A flowchart is shown in Figure 7 that demonstrates the gear selection process. A set of control logics receives information related to the vehicle speed, road grade, and vehicle acceleration, and it evaluates these values against pre-defined upper and lower bounds of these parameters respectively. Next, it is checked whether the current values of the three parameters satisfy the upshift or downshift condition or hold the current gear.

It is assumed that the vehicle starts on gear 1. At every instance, the upper and lower range of the vehicle speed (i.e., up_speed and down_speed), road grade (i.e., up_grd and down_grd), and acceleration (i.e., up_acc and down_acc) are determined according to the current vehicle speed and gear number. Then, the current values of these parameters will be compared with either the upper range of all parameters

respectively for upshift if the current gear is on gear 1 or the lower range of all parameters respectively for downshift if the current gear is on gear 2. The controller's decision could be either to change gear (upshift/downshift) or to stay on the current gear. However, in case of more than two gears in the transmission system, current parameter values are compared with both the upper and lower bounds for all middle gears i.e., the 2nd gear in a three-speed transmission system or the 2nd gear and 3rd gear in a four-speed transmission system, and so on. A minimum waiting period or shift interval is maintained between every consecutive gearshift to avoid frequent gear shifting as well as to ensure riding comfort. The shift interval must be greater than the maximum gearshift time, because the gearshift time is not necessarily the same for every gear change in a transmission system with more than two gears for both upshift and downshift [36,49]. Based on the study conducted by Zhang et al. [46], a minimum shift interval of 4 s is assumed to be sufficient for an acceptable level of riding comfort. It has been found through simulation that higher shift interval time leads to energy consumption. For example, increasing shift interval time from 1 to 4 s costs 1–1.5% additional energy consumption depending on different drive cycles.

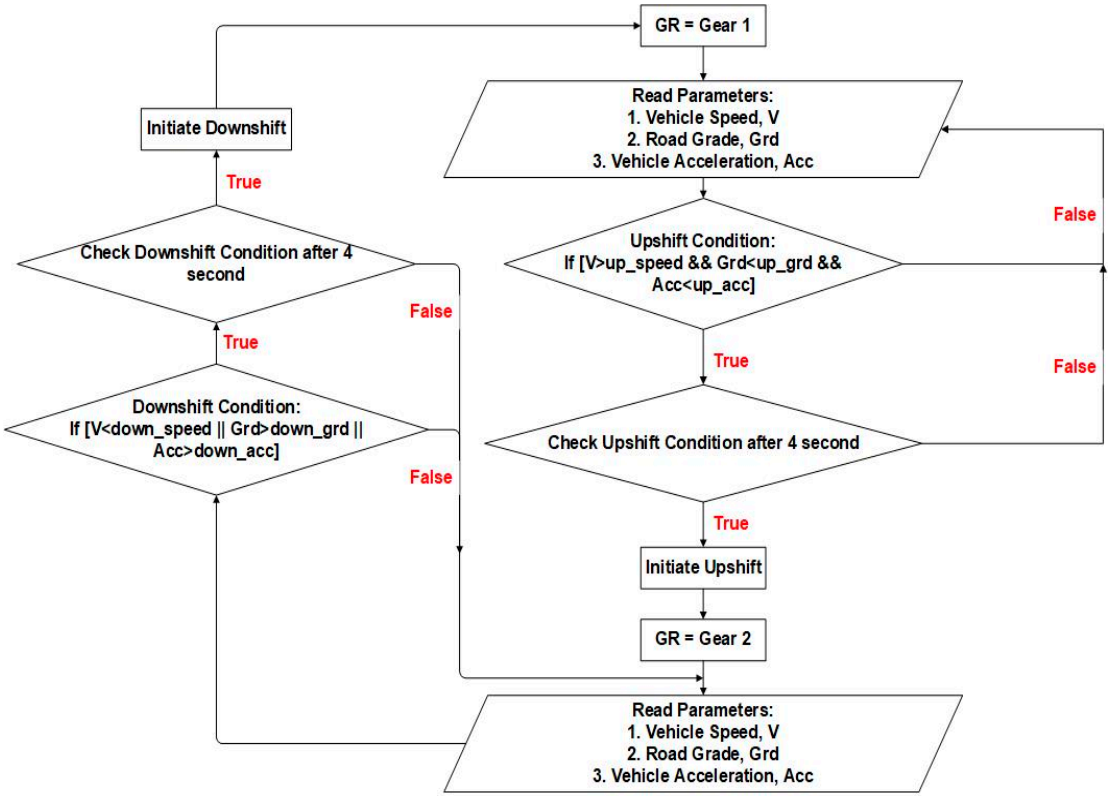

Figure 7. Gearshift control logic for an EV with a two-speed transmission system.

4. Optimization Method

It is evident in the literature that each set of gear ratios is associated with a certain gearshift schedule that can ensure minimum energy consumption. In other words, it can be said that the gear ratios and gearshift strategy are mutually associated to achieve the desired vehicle dynamic and economic performances. In this study, both the gear ratios and gearshift schedule are optimized combinedly in the optimization process. Table 6 shows some approaches or methods of optimization of the multi-speed transmission system in EVs in recent studies. All these methods are generally known as global optimization methods that are computationally intensive [13]. The global optimization method can generate more accurate results than the results achieved from the optimization method suitable for the local minimum value of the objective function. However, it is not shown how much more accurate results or benefits can be made through using global methods compared to those by using methods for

local minimum values in this problem. In this study, both global and local optimization methods will be implemented to search for optimal gear ratios of the two-speed transmission system in EV, and then, the results will be compared.

Table 6. Approaches for optimization of gear ratios in the multi-speed transmission system in EVs.

Optimization Method	Cost Function	Decision Variables	Constraints
Multi-Objective Genetic Algorithm [7]	Overall energy consumption Acceleration time, $t_{0–100}$ sec	Gear ratios	Step ratio: 1.9
Dynamic Programming [4]	Energy consumption in terms of ΔSOC	Gear ratios	Max. speed, Grade ability, Step ratio: 1.7–1.8
Auto Search Method [9]	Driving range	Gear ratios and shift schedule	Step ratio: 3.4
Genetic Algorithm [13]	Mean motor efficiency Driving range	Gear ratios and shift schedule	Max. speed, Grade ability, Acceleration time
Genetic Algorithm [14]	Energy consumption in terms of driving range	Gear ratios	Max. speed, Grade ability, Acceleration time
Brute Force Iterative Algorithm [2]	Acceleration time, Grade ability, Top speed, Energy consumption	Gear ratios	Step ratio, Max. speed, Grade ability, Acceleration time
Brute Force Iterative Algorithm [15]	Acceleration time, Grade ability, Top speed, Energy consumption	Gear ratios	Step ratio, Max. speed, Grade ability, Acceleration time

Gradient descent (GD) and pattern search (PS) methods are implemented to optimize the gear ratios and shift schedule of the two-speed transmission system of the EV model, and next, the results obtained from these methods are compared. Both methods can handle multi-variables and multiple objectives or cost functions. However, the GD method using the sequential quadratic programming algorithm is appropriate for optimization problems with the local minimum value of objective functions [50]. This method has the flexibility to consider any values of control variables within the bounds during each iteration, even the values on the boundary of variables. To the other end, the PS method is a derivative-free method to find the optimum solution and can handle discontinuous functions [51]. The PS method can be implemented to both global and local search. With a good initial start point, PS can provide a better global solution and may require a reduced computational time compared to the other traditional global optimization method i.e., evolutionary programming and genetic algorithm. To conduct the optimization, two objectives have been considered; one is the energy consumption in a complete drive cycle, and the other is the tracking error between the drive cycle input speed and vehicle output speed. The optimization problem is to find the minimum values of the objective functions for the desired set of gear ratios and optimized gearshift schedules in relation to vehicle acceleration and road grade.

4.1. Problem Formulation

In the optimization problem, state variables are represented by the objective functions i.e., energy consumption over the entire drive cycle and tracking error.

$$F_{obj} = min(f_1,\ f_2) \tag{11}$$

$$f_1 = E_{dc} = \int_0^t P_M\, dt \tag{12}$$

$$f_2 = max(\,V_{in}\ \sim V_{out}) \tag{13}$$

In Equations (11) and (12), f_1 *or* E_{dc} stands for the total energy consumption in a complete drive cycle, where P_M is the required motor output power at the time step, dt, and t is the end time of the drive cycle. The motor output power, P_M, is the summation of the required mechanical power, P_{Mech}, at the input side of the transmission system to run the vehicle and motor loss, P_{Loss}, corresponding to the motor torque, T_M, and speed, n_M, as shown in Equation (10). The motor efficiency, η_M, is recalled from the lookup table during the simulation. In Equations (11) and (13), f_2 represents the tracking error between the input drive cycle speed, V_{in}, and output vehicle speed, V_{out}. NEDC and UDDS drive cycles are used as the input to the EV model. The aim of the optimization is to minimize the values of these two objectives and to find out the corresponding values of gear ratios along with the optimal gearshift schedule.

$$u = \in (GR_1,\ GR_2,\ k_1, k_2,\ k_3, k_4) \tag{14}$$

The control variable u in Equation (14) includes gear ratios i.e., GR_i, and shift factors i.e., k_i, for both shifting maps in relation to vehicle acceleration and road grade for the upshift and downshift lines, respectively. Shift factors are introduced in such a way that these would optimize the gearshift lines within the middle region of both gearshift schedule maps i.e., around the 30 km/h to 70 km/h speed range of Figure 5 and around the 20 km/h to 80 km/h speed range of Figure 6. Since gear selection is obvious (i.e., either gear 1 or gear 2) on either side of the middle region of both schedules, these areas have been excluded in the optimization process. It is expected that this measure would eliminate some unnecessary computation during the optimization.

4.2. Boundary Conditions and Constraints

The upper and lower bound of gear ratios are set based on the target performances as presented in Table 5. The lower bound of the 1st gear ratio is determined by the maximum gradeability requirement and can be found using Equation (15).

$$\left.\begin{aligned} GR_{1min} &= \frac{Vehicle\ Resistance\ Force\ at\ Const.\ Max.\ Speed\ at\ Max.\ Gradeability * Wheel\ Radius}{Effective\ Motor\ Torque} \\ GR_{1min} &= \frac{(m*g*(\mu*\cos\theta_{max}+\sin\theta_{max})+0.5*C_d*\rho*A*(V\_grd_{max}/3.6)^2)*r_w}{T_{Mmax}*\eta_{PT}} \end{aligned}\right] \tag{15}$$

The upper bound of the 2nd gear ratio is set based on the maximum vehicle speed requirement and is calculated according to Equation (16).

$$\left.\begin{aligned} GR_{2max} &= \frac{Maximum\ Motor\ Speed * Wheel\ Radius}{Maximum\ Vehicle\ Speed} \\ GR_{2max} &= \frac{(2*\pi*n_{max}/60)*r_w}{V_{max}/3.6} \end{aligned}\right] \tag{16}$$

However, it is necessary to check whether the motor can generate enough torque required to run the vehicle at maximum speed. Equation (17) shows the torque ratio between the vehicle resistance torque at the desired top speed and the maximum motor torque at the maximum motor speed i.e.,

$$\left.\begin{aligned} \gamma &= \frac{Vehicle\ Resistance\ Torque\ at\ Maximum\ Speed}{Maximum\ Motor\ Torque\ at\ Maximum\ Motor\ Speed} \\ \gamma &= \frac{(m*g*(\mu*\cos\theta+\sin\theta)+0.5*C_d*\rho*A*(V_{max}/3.6)^2)*r_w}{T_{Mmax}\ at\ n_{max}} \end{aligned}\right]. \tag{17}$$

GR_{2max} will be acceptable under the condition of $\gamma \leq GR_{2max}$ i.e., enough motor torque will be available at the vehicle's top speed. To set the upper bound of the 1st gear ratio, GR_{1max}, and the lower bound of the 2nd gear ratio, GR_{2min}, the idea of step ratio will be applied. Step ratio (str), is the ratio between two consecutive gear ratios. The maximum step ratio is set to 3.4 based on a study conducted by Zhou et al. [9]. Now, GR_{1max} and GR_{2min} can be estimated by using Equation (18) i.e.,

$$\begin{aligned} GR_{1max} &= GR_{2max} * 3.4 \\ GR_{2min} &= GR_{1min}/3.4. \end{aligned} \tag{18}$$

Considering the above-mentioned assumptions and the vehicle parameters presented in Table 2, the range of both gear ratios, as shown in Equation (19), can be found with imposing the requirement of $\frac{GR_1}{GR_2} \leq 3.4$ *or* $GR_1 - 3.4 * GR_2 \leq 0$.

$$\begin{array}{c} 8.23 \leq GR_1 \leq 20.51 \\ 2.42 \leq GR_2 \leq 6.03 \end{array} \quad (19)$$

It has been mentioned in the earlier section that the traditional approach of imposing the weighting factor to create a buffer zone between the upshift and downshift lines has been considered as a primary guideline. In line with that, a 20% limit as shown in Equation (20) is set for each shifting line to move or shift either downward or upward from its primary position.

$$0.80 \leq k_i \leq 1.20 \quad (20)$$

$$GR_1 - str \times GR_2 \leq 0 \quad (21)$$

$$\left(2 \times \pi \times \frac{n_{up}}{60}\right) \times 3.6 \times r_w \div GR_1 - \left(2 \times \pi \times \frac{n_{down}}{60}\right) \times 3.6 \times r_w \div GR_2 > c \quad (22)$$

$$k_1 - k_2 \leq 0 \quad (23)$$

$$k_3 - k_4 \leq 0 \quad (24)$$

Apart from the boundary conditions, four additional constraints are set out in Equations (21)–(24) to prevent the generation of an unacceptable combination of control variables in the optimization, even if the values are within the defined boundary of each variable separately. As in Equation (21), a maximum limit of the step ratio, *str*, needs to be ensured to avoid an undesirable shift jerk or shock load on the gears during gearshift as well as riding discomfort. The maximum step ratio, *str*, is considered 3.4 as mentioned earlier in this section. The second constraint in Equation (22) ensures the difference between the vehicle upshift speed $@GR_1$ in km/h and downshift speed $@GR_2$ in km/h above a certain value, *c*, to prevent the gear hunting problem while *c* can be any small positive number i.e., 5 or less, etc. In other words, a higher value of *c* may have a negative impact on energy consumption. The third and fourth constraints in Equations (23) and (24) are about providing the flexibility of moving both upshift and downshift lines up to 20% downward or upward direction from its original position, while the buffer zone should not be less than that of the primary gearshift maps associated with the vehicle acceleration and road grade, respectively.

5. Simulation and Result Analysis

Simulation has been conducted on the EV model with a two-speed transmission system in the MATLAB/Simulink environment. All the powertrain components are connected within a forward-facing model as shown in Figure 8, while only the battery is connected to the electric motor as a backward-facing module to show the drop in battery state-of-charge. The EV model is developed based on the Powertrain Blockset library available in the Simulink library browser. The Stateflow library is employed to construct the gearshift control logic as outlined in Figure 7.

Optimization has been conducted in two phases. The gear ratios and the gearshift map in relation to vehicle acceleration are optimized in the first phase. Next, the gearshift schedule for the road grade is optimized separately because the available drive cycles are based on a flat road. To evaluate the vehicle performances, a standard driving scenario on a frequently changing road grade is not readily available. Tan et al. [16] presented a driving cycle with associated road grade information in their study. However, that driving scenario is applicable to dump trucks that operated on a very specialized structured route in the mining zone. In this study, customized road grade information is considered on a standard drive cycle to evaluate the primary gearshift schedule in relation to the road grade for the two-speed transmission system in an EV model.

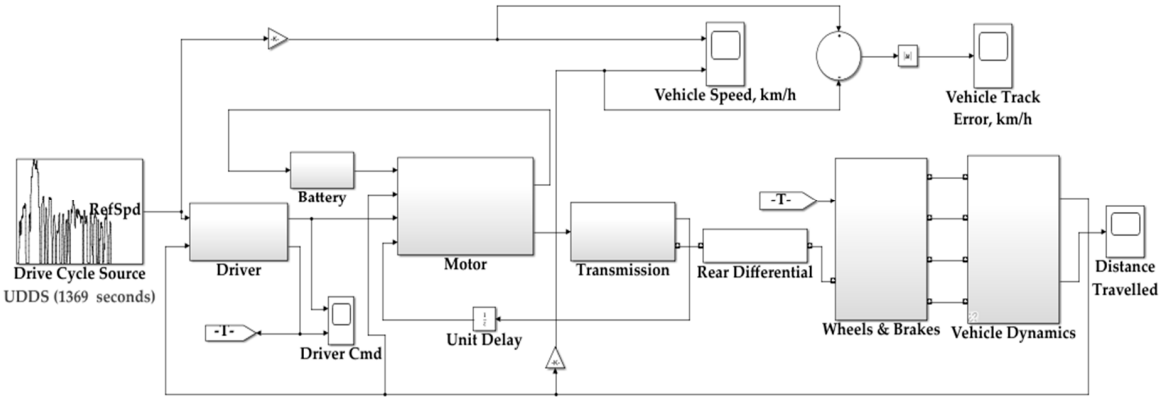

Figure 8. EV model layout within the MATLAB/Simulink platform.

5.1. Optimization of Gear Ratios and Gearshift Schedule for Vehicle Acceleration

Figure 9 displays NEDC and UDDS drive cycles that are used as the input to the EV model. In this phase, optimization is conducted considering two groups of control variables where only gear ratios are considered as the first group of control variables and both the gear ratios and shift factors of the shift map for acceleration are considered combinedly as the second group of control variables for each drive cycle. Being a global optimization method, for the second group of control variables, the PS method takes an excessively longer duration to conduct the optimization. To accelerate the optimization process, an exception is made to avoid the inconvenience of uncertain waiting time, and each set of control variables are optimized separately through the PS method A set of generic gear ratios i.e., 10.00 for GR_1 and 5.20 for GR_2, have been considered to start the simulation. The initial value of each shift factor of the gearshift map for vehicle acceleration is set to 1.0 to ensure that the primary gearshift maps are considered at the beginning of the optimization process.

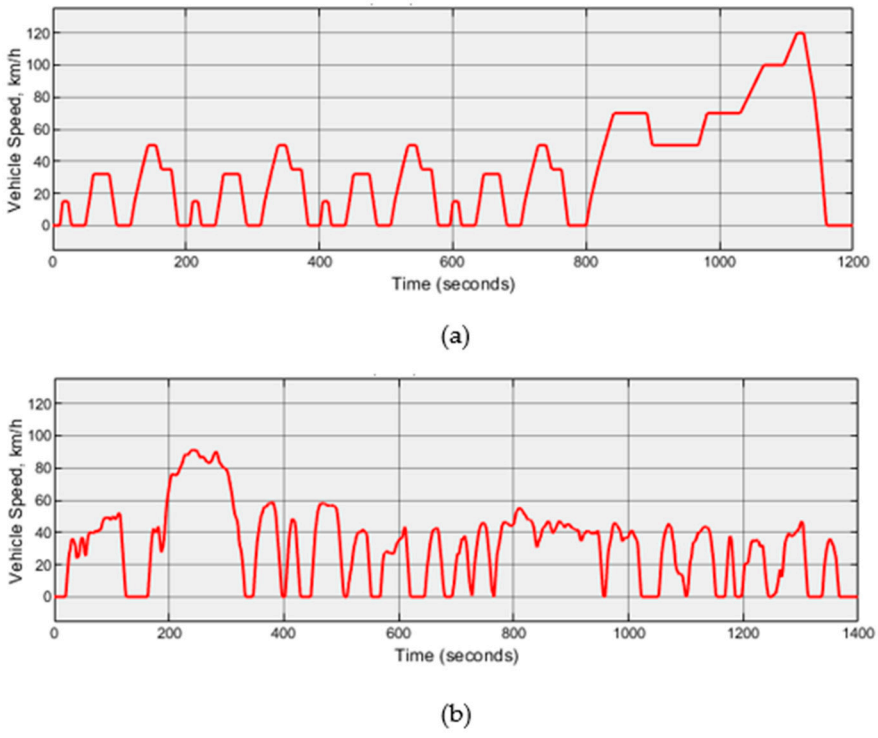

Figure 9. Vehicle driving conditions: (**a**) NEDC—New European Drive Cycle and (**b**) UDDS—Urban Dynamometer Driving Schedule.

It has been noticed that the maximum tracking error is around 4 km/h for NEDC and 6.4 km/h for the UDDS drive cycle with optimized gear ratios as presented in Figure 10a,b respectively. Table 7 shows the energy consumption of the two-speed EV model before and after optimization on complete NEDC and UDDS drive cycles.

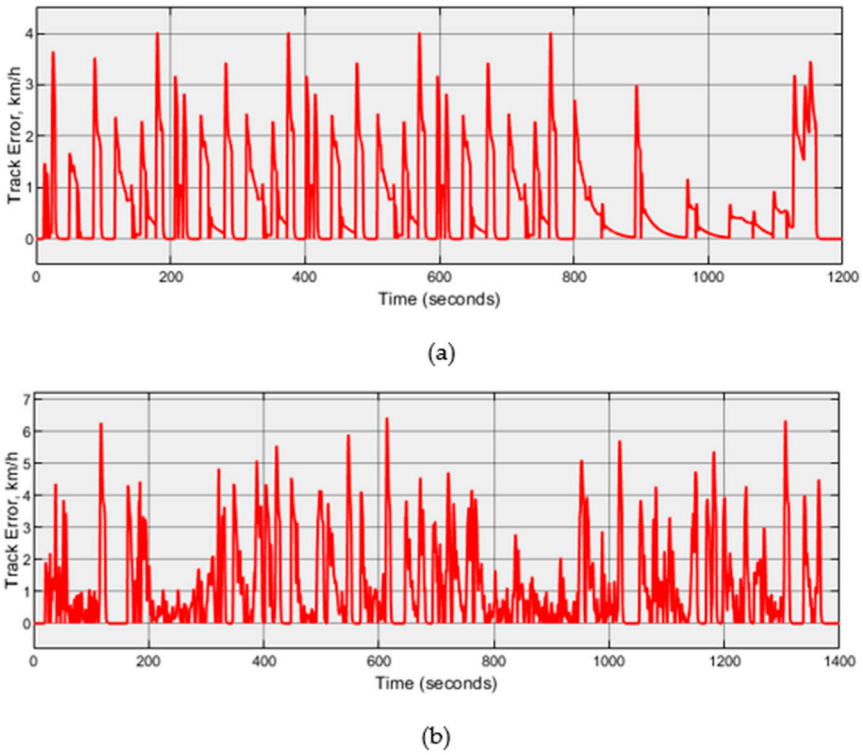

Figure 10. Vehicle tracking error for EV with a two-speed transmission system on: (**a**) NEDC and (**b**) UDDS drive cycles.

Table 7. Optimization of gear ratios and gearshift schedule in relation to vehicle acceleration of a two-speed transmission system in the EV model on the NEDC and UDDS drive cycles.

Drive Cycle	Optimization Method	Control Variables and Objective Function before/after Optimization						
		Gear Ratios		Shift Factor for Acceleration (Down/Up)		Energy Consumption, MJ		
		Before	After	Before	After	Before	After	Improvement
NEDC	Pattern Search	10.00/5.20	8.24/4.9364	1.0/1.0	-	2.9968	2.8763	4.0210%
	Gradient Descent		8.24/4.9352		-		2.8762	4.0243%
	Pattern Search	8.24/4.9364	-	1.0/1.0	1.0107/0.9337	2.8763	2.8755	0.0278%
	Gradient Descent	10.00/5.20	8.24/4.9352		1.2/1.2	2.9968	2.8586	4.6116%
UDDS	Pattern Search	10.00/5.20	8.24/4.9364	1.0/1.0	-	3.9117	3.7224	4.8393%
	Gradient Descent		8.24/4.9352		-		3.7223	4.8419%
	Pattern Search	8.24/4.9364	-	1.0/1.0	1.1494/1.1480	3.7224	3.7191	0.0887%
	Gradient Descent	10.00/5.20	8.24/4.9352		1.2/1.2	3.9117	3.7178	4.9569%

Several more observations can be made based on the results achieved through the optimization process.

- After optimization, both GD and PS methods offer almost similar improvements in terms of energy consumption i.e., 4–5% less energy consumption depending on the driving scenarios i.e., NEDC or UDDS, as plotted in Figure 11. Another reflection from the results in Table 7 is that compared to the impact on the energy consumption by the shift factors of the shifting map for acceleration, gear ratios play more dominating roles on vehicle economic performance.

- For both driving scenarios i.e., NEDC and UDDS, optimized gear ratios achieved through both GD and PS methods are practically the same with little difference (approximately 0.02%) in the second gear ratio. To the other end, the shift factors of the gearshift map for vehicle acceleration are same for the GD methods on either driving conditions, while some difference can be noticed in the results through the PS method.
- A significant observation is that both optimization methods tried to move the gear ratios toward the lower bound of each gear ratio. This indicates that the lower value of gear ratios will contribute to economic driving. However, further lowering the value of gear ratios has been restricted by dynamic performance targets. Secondly, an upward move (20% for the GD method and nearly 15% for the PS method) based on the results in Table 7 of both upshift and downshift lines of the gearshift schedule for acceleration is experienced after optimization, while the buffer zone of primary gearshift schedule is maintained as illustrated in Figure 12. An exception with the PS method i.e., close to the primary gearshift schedule with a slightly wider buffer zone, is observed after optimization with the NEDC driving cycle. Although shift factors for vehicle acceleration have relatively less impact on energy consumption, the results could be viewed as a guideline to generate the primary gearshift schedule with more confidence.

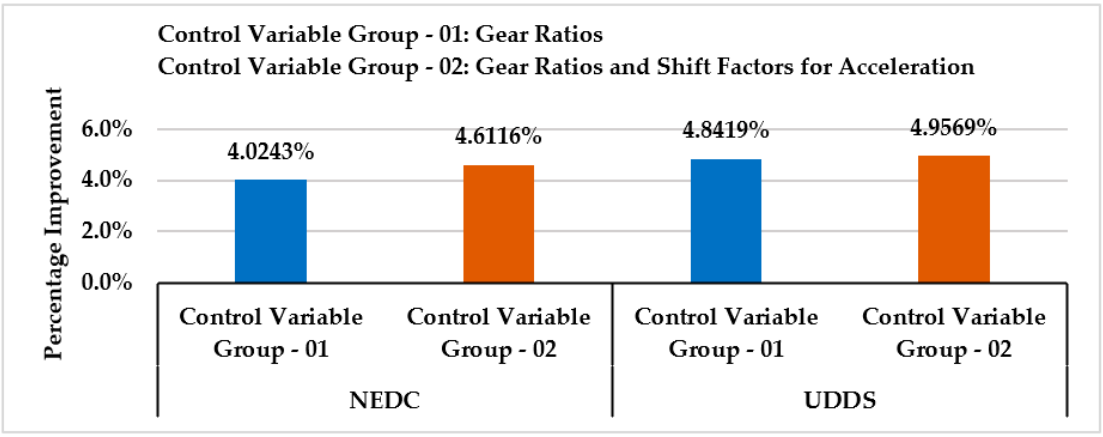

Figure 11. Energy-saving through optimization of gear ratios and shift factors of a gearshift schedule for acceleration combinedly for a two-speed transmission system in an EV model on NEDC and UDDS drive cycles.

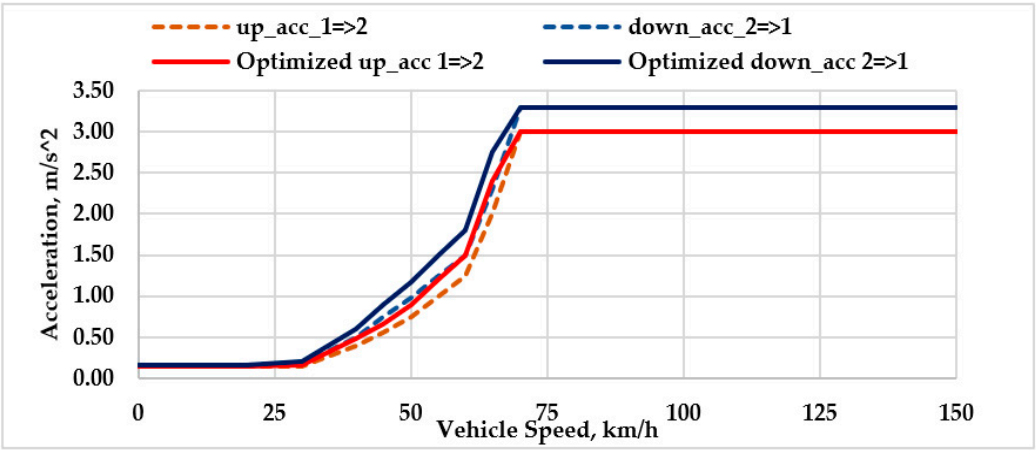

Figure 12. Gearshift schedule in relation to vehicle acceleration before and after optimization.

5.2. Optimization of Gearshift Schedule for Road Grade

It is mentioned earlier that a standard driving scenario with a frequently varied road grade has not been found in the literature. Therefore, to evaluate the primary gearshift map for a road grade, the Economic Commission for Europe (ECE, Geneva, Switzerland) Extra-Urban driving cycle is chosen because this drive cycle covers a wider speed range from low to relatively high with reasonable speed variations, as shown in Figure 13a. The low-speed region of this drive cycle is associated with a higher road grade, and the high-speed region is associated with a lower road grade, as shown in Figure 13.

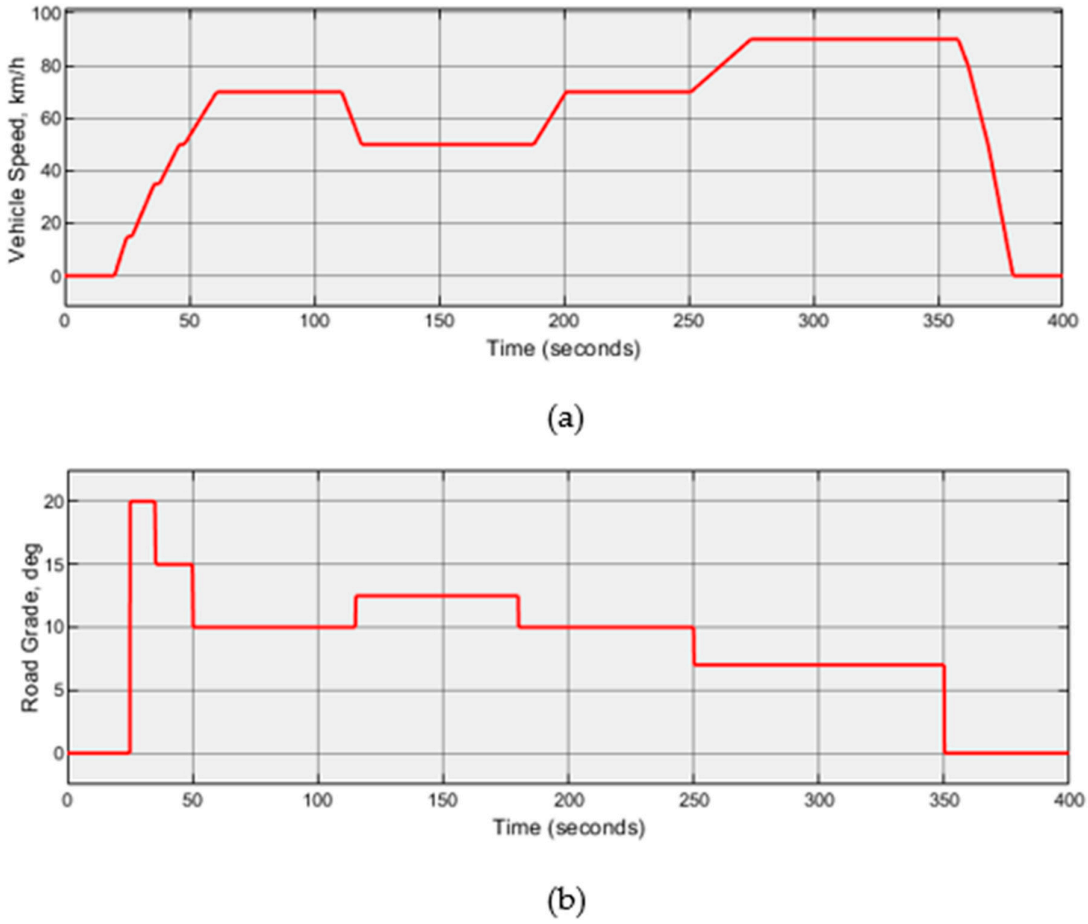

Figure 13. Vehicle input speed associated with road grade information: (**a**) Economic Commission for Europe (ECE) Extra-Urban driving cycle and (**b**) Road grade distribution.

In this phase of optimization, the first group of control variables comprises both generic gear ratios as well as the shift factors of both primary gearshift maps for vehicle acceleration and road grade at the beginning of optimization. The second group of control variables contains only the shift factors of a shifting map for road grade considering the fixed and previously optimized values of gear ratios and shift factors of a shifting map for vehicle acceleration. Figure 14a shows the deviation in vehicle speed tracking (i.e., around 5.5 km/h), which is similar or close to that deviation on flat road scenarios, as shown in Figure 10. Another observation in Figure 14b,c is that the first gear selection in the mid-region (i.e., between 120 s to 180 s) of the drive cycle is altered after optimization, and the second gear is chosen throughout most of the driving time. The optimization results are demonstrated in Table 8.

Energy saving through optimization is evident in Figure 15. The optimized gearshift schedule in relation to road grade shows a significant contribution to vehicle driving economy compared to the combined dominance through optimized gear ratios and gearshift schedule for vehicle acceleration.

An overall assessment of all the results of optimization in this study reflects that the gear ratios and gearshift schedule for the uphill driving scenario could be considered as the key parameters that have a major influence on the vehicle economic performance.

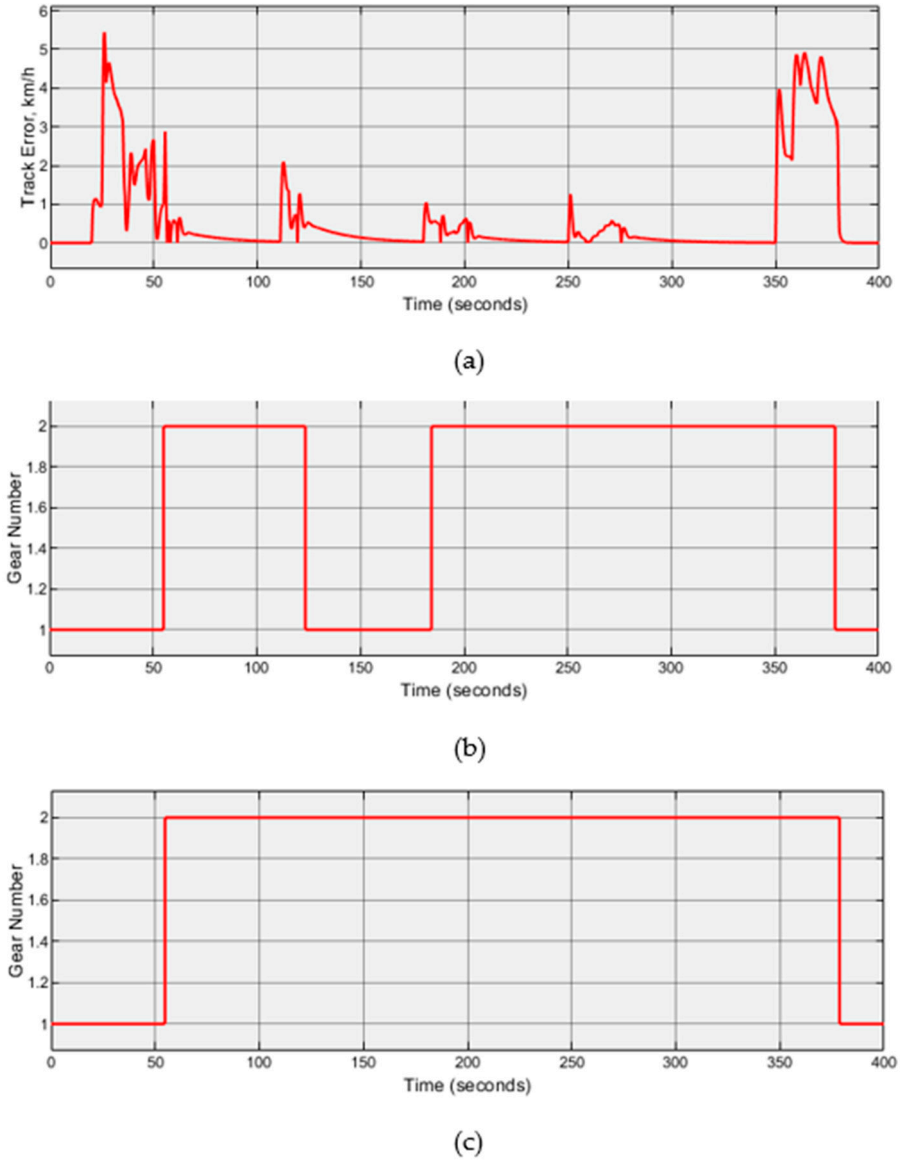

Figure 14. ECE Extra-Urban driving cycle on uphill driving conditions: (**a**) Tracking response; (**b**) Gear distribution before optimization and (**c**) Gear distribution after optimization.

Table 8. Optimization of gearshift schedule in relation to road grade of two-speed transmission system in an EV model on ECE Extra-Urban driving cycle associated with road grade information.

Drive Cycle	Optimization Method	Control Variables and Objective Functions before/after Optimization								
		Gear Ratios		Shift Factor for Acceleration (Down/Up)		Shift Factor for Grade (Down/Up)		Energy Consumption, MJ		
		Before	After	Before	After	Before	After	Before	After	Improvement
ECE Extra-Urban Driving Cycle	Pattern Search	10.00/5.20	9.887/6.04	1.0/1.0	-	1.0/1.0	-	13.024	13.115	−0.700%
	Gradient Descent		8.24/4.935		1.2/1.2		1.195/1.195		12.057	7.422%
	Pattern Search	8.24/4.935	-	1.0/1.0	1.127/1.113	1.0/1.0	-	12.601	12.601	0.00%
	Pattern Search	8.24/4.935	-	1.2/1.2	-	1.0/1.0	1.127/0.966	12.598	12.057	4.290%
	Gradient Descent		-		-		1.2/1.2		12.057	4.290%

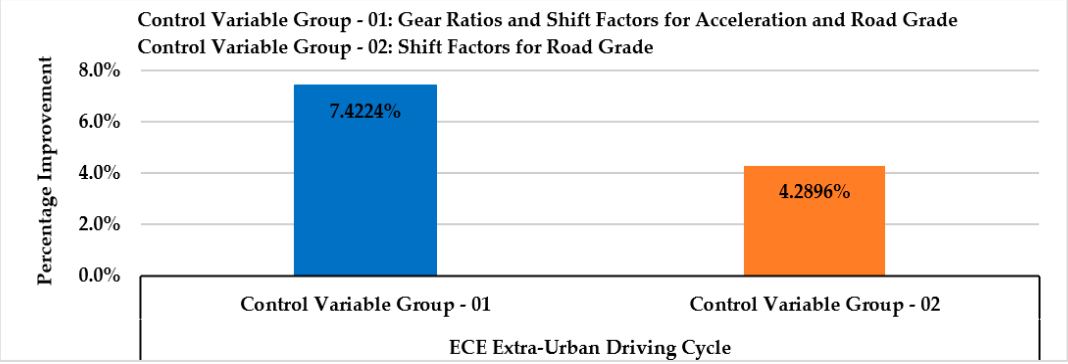

Figure 15. Energy saving through the optimization of gear ratios and shift factors of a gearshift schedule for acceleration and road grade for a two-speed transmission system in an EV model on the ECE Extra-Urban driving cycle with varied road grade.

It is apparent from the results in Tables 7 and 8 that both the GD and PS methods generate almost similar optimized gear ratios and shift factors of gearshift schedule in relation to vehicle acceleration with some exceptions. In Table 8, optimized gear ratios through the PS method can be ignored because for all other cases, similar gear ratios as well as energy savings are experienced after optimization. For uphill driving conditions, some difference is found on the optimized gearshift schedule, although the equivalent amount of energy-saving is observed with both optimization methods. An optimized gearshift schedule through the GD method is shifted 20% in the upward direction from the primary position, while the optimized downshift and upshift lines through the PS method are shifted around 12.73% upward and 3.42% downward, respectively, from the primary position. In other words, the buffer zone is further widened through the PS optimization method, as shown in Figure 16, while having similar energy-saving achieved through the GD method.

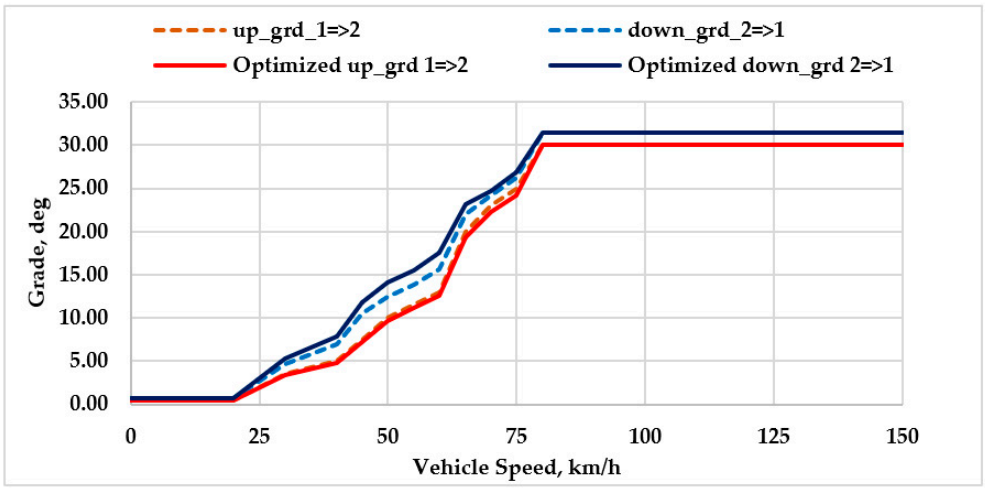

Figure 16. Gearshift schedule in relation to road grade before and after optimization.

It should be remembered that the road grade information associated with the ECE Extra-Urban driving cycle is not from any recognized source; rather, this driving scenario is implemented in this study to see how vehicle driving economy is impacted by the frequently changing road grade. Therefore, without focusing on the specific numerical results, it would be wise to emphasize what message these results are producing. On that note, an upward shift of the gearshift schedule for both the case with vehicle acceleration and road grade could have a positive impact on energy saving with a multi-speed transmission system in EV that would be further validated through the experiments to draw a more specific conclusion.

5.3. Comparison of Results with Conventional Approach

To have a comprehensive understanding, it is necessary to evaluate the proposed gearshift strategy with the conventional rule-based gearshift strategy. On that note, two gearshift schedules as shown in Figure 17a,b are chosen from two studies published by Ruan et al. [11] and Zhu et al. [8], respectively. It is understandable that the assumptions are not necessarily the same in every study. However, a similar vehicle size is assumed to be worth consideration as a basis to compare the performances of these gearshift strategies.

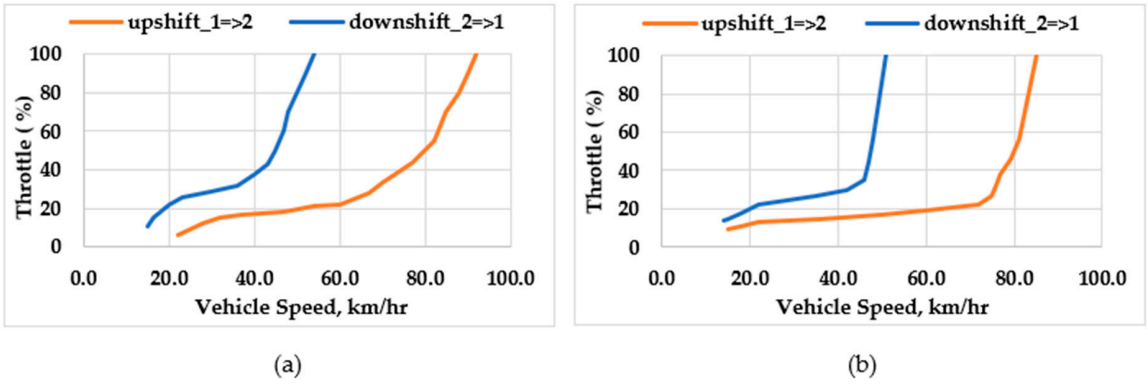

Figure 17. Conventional rule-based (i.e., throttle or torque demand and vehicle speed) gearshift strategy: (**a**) gearshift strategy—01 [11] and (**b**) gearshift strategy—02 [8].

Significant findings can be drawn from Figure 18. Around 3.0–4.2% and 3.7–3.9% less energy is consumed on NEDC and UDDS drive cycles respectively with a conventional gearshift schedule compared to that with the proposed gearshift schedule. However, the proposed gearshift strategy on uphill driving conditions can save energy up to 17.7% compared to that with the conventional approach. Although these results may vary slightly based on other considerations (i.e., EV powertrain components specifications, efficiency etc.), it is revealed that the proposed gearshift strategy could respond effectively to changing driving conditions, especially in hilly driving conditions, and it can also offer better economic performance.

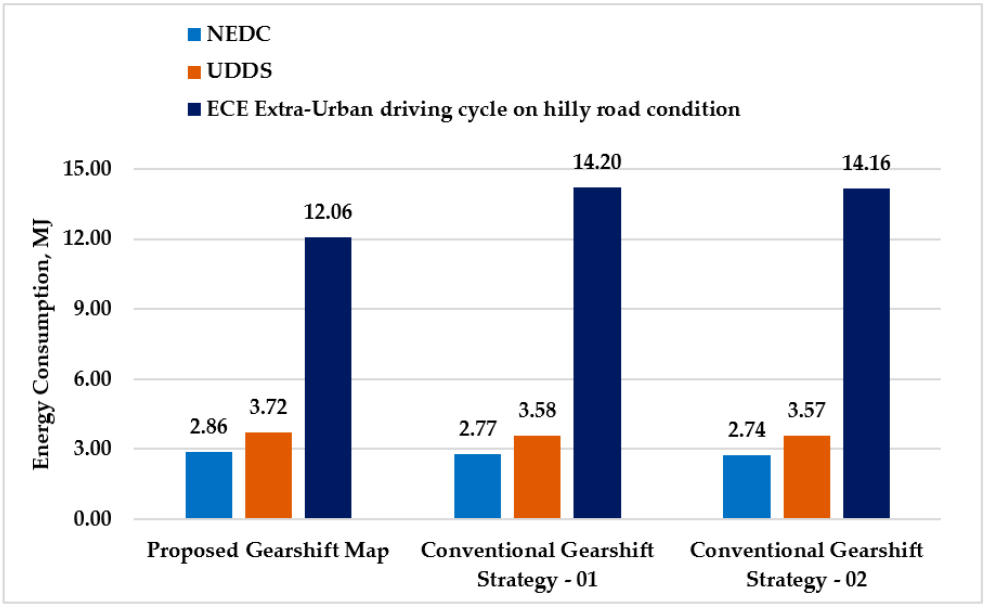

Figure 18. Comparison of energy consumption between proposed and conventional gearshift strategies.

6. Conclusions

A novel gearshift schedule has been presented and explained in the first part of this study. While meeting up the dynamic performance requirements, this gearshift schedule technique is expected to select the appropriate gear in relation to acceleration demand and change in road grade. Next, the gear ratios of a two-speed transmission system in EV and a gearshift schedule for both vehicle acceleration and road grade are optimized combinedly through two optimization methods i.e., GD and PS methods. After optimization of the two-speed transmission system, around 4% to 7.5% energy saving has been found, depending on the different driving scenarios considering both flat road and uphill road conditions, according to the results in Tables 7 and 8. Contributions on energy economy through the gear ratios and gearshift schedule for both vehicle acceleration and road grade have been assessed separately. It is revealed that compared to the impact of the gearshift schedule for acceleration, gear ratios play more dominating roles on vehicle energy consumption on flat road conditions. In uphill driving scenarios, the impact of gearshift schedule in relation to road grade on vehicle economic performance can even be more than the combined effect of gear ratios and gearshift map for acceleration. Apart from this, a comparison is conducted on the performance between the proposed gearshift strategy and the conventional approach. It is found that the proposed gearshift strategy shows a better response on hilly road compared to that with a conventional rule-based gearshift strategy.

The next significant finding of this study is about how the gear ratios and gearshift schedules are tuned after the implementation of optimization methods. It is observed that the values of both gear ratios are moving toward their lower boundaries based on the results in Tables 7 and 8 after optimization, while the primary gearshift schedule for vehicle acceleration is shifted in the upward direction, extending the working area of the second gear, as revealed in Figure 12. For the uphill driving conditions, the primary gearshift schedule in relation to the road grade has been shifted in the upward direction after optimization through the GD method, similar to that observed with the shifting map for acceleration. However, the gearshift schedule with a wider buffer zone is observed after implementing the PS method with equivalent energy consumption as found through implementing the GD method. Through this analysis, it has been explained how the shifting of gearshift schedule lines has an impact on the energy consumption of EVs with a multi-speed transmission system.

Author Contributions: All authors were involved throughout the development process of this research article. Individual contributions can be stated as Conceptualization, M.E. and M.R.A.; methodology, M.E. and M.R.A.; software, S.G. and M.R.A.; optimization and result analysis, M.R.A.; writing—original draft preparation, M.R.A.; writing—review and editing, M.E., S.G. and M.R.A.; supervision, M.E. and S.G. All authors have read and agreed to publish this version of the manuscript.

Funding: Australian Government Research Training Program (RTP) supported this research.

Conflicts of Interest: The authors declare no conflict of interest.

Abbreviations

Following abbreviations are used in this manuscript.

AMT	Automatic Mechanical/Manual Transmission
GD	Gradient Descent
GR	Gear Ratio
ECE	Economic Commission for Europe
EV	Electric Vehicle
MJ	Mega-Joule
NEDC	New European Driving Cycle
PS	Pattern Search
SOC	State-of-Charge
UDDS	Urban Dynamometer Driving Schedule

References

1. Ahssan, M.R.; Ektesabi, M.M.; Gorji, S.A. Electric Vehicle with Multi-Speed Transmission: A Review on Performances and Complexities. *SAE Int. J. Altern. Powertrains* **2018**, *7*, 169–181. [CrossRef]
2. Sorniotti, A.; Boscolo, M.; Turner, A.; Cavallino, C. Optimization of a Multi-Speed Electric Axle as a Function of the Electric Motor Properties. In Proceedings of the 2010 IEEE Vehicle Power and Propulsion Conference, Lille, France, 1–3 September 2010; pp. 1–6. [CrossRef]
3. Sorniotti, A.; Subramanyan, S.; Turner, A.; Cavallino, C.; Viotto, F.; Bertolotto, S. Selection of the Optimal Gearbox Layout for an Electric Vehicle. *SAE Int. J. Engines* **2011**, *4*, 1267–1280. [CrossRef]
4. Gao, B.; Liang, Q.; Xiang, Y.; Guo, L.; Chen, H. Gear Ratio Optimization and Shift Control of 2-Speed I-AMT in Electric Vehicle. *Mech. Syst. Signal. Process.* **2014**, *50–51*, 615–631. [CrossRef]
5. Tian, S.; Wang, Y.; Wu, L. Parameters Matching and Effects of Different Powertrain on Vehicle: Performance for Pure Electric City Bus. In Proceedings of the SAE 2015 Commercial Vehicle Engineering Congress, Rosemont, IL, USA, 6–8 October 2015. [CrossRef]
6. Zhou, X.X.; Walker, P.D.; Zhang, N.; Zhu, B.; Ding, F. The influence of transmission ratios selection on electric vehicle motor performance. In Proceedings of the ASME 2012 International Mechanical Engineering Congress and Exposition, Houston, TX, USA, 9–15 November 2012; pp. 289–296. [CrossRef]
7. Morozov, A.; Humphries, K.; Zou, T.; Martins, S.; Angeles, J. Design and Optimization of a Drivetrain with Two-Speed Transmission for Electric Delivery Step Van. In Proceedings of the 2014 IEEE International Electric Vehicle Conference, Florence, Italy, 17–19 December 2014; pp. 1–8. [CrossRef]
8. Zhu, B.; Zhang, N.; Walker, P.; Zhou, X.; Zhan, W.; Wei, Y.; Ke, N. Gear Shift Schedule Design for Multi-Speed Pure Electric Vehicles. *Proc. Inst. Mech. Eng. Part. D Int. J. Automot. Mech. Eng.* **2015**, *229*, 70–82. [CrossRef]
9. Zhou, X.; Walker, P.; Zhang, N.; Zhu, B. Performance Improvement of a Two Speed EV through Combined Gear Ratio and Shift Schedule Optimization. In Proceedings of the SAE 2013 World Congress & Exhibition, Detroit, MI, USA, 16–18 April 2013. [CrossRef]
10. Ruan, J.G.; Walker, P.D.; Wu, J.L.; Zhang, N.; Zhang, B.J. Development of Continuously Variable Transmission and Multi-Speed Dual-Clutch Transmission for Pure Electric Vehicle. *Adv. Mech. Eng.* **2018**, *10*, 1687814018758223. [CrossRef]
11. Ruan, J.; Walker, P.; Zhang, N. A Comparative Study Energy Consumption and Costs of Battery Electric Vehicle Transmissions. *Appl. Energy* **2016**, *165*, 119–134. [CrossRef]
12. Saini, V.; Singh, S.; Shivaram, N.V.; Jain, H. Genetic Algorithm Based Gear Shift Optimization for Electric Vehicles. *SAE Int. J. Altern. Powertrains* **2016**, *5*, 348–356. [CrossRef]
13. Walker, P.D.; Rahman, S.A.; Zhu, B.; Zhang, N. Modelling, Simulations, and Optimisation of Electric Vehicles for Analysis of Transmission Ratio Selection. *Adv. Mech. Eng.* **2013**, *5*, 340435. [CrossRef]
14. Yin, Q.; Wu, Z.; Rui, X. Parameter Design and Optimization of Electric Vehicle. In Proceedings of the 2014 IEEE Conference and Expo Transportation Electrification Asia-Pacific, Beijing, China, 31 August–3 September 2014; pp. 1–7. [CrossRef]
15. Di Nicola, F.; Sorniotti, A.; Holdstock, T.; Viotto, F.; Bertolotto, S. Optimization of a Multiple-Speed Transmission for Downsizing the Motor of a Fully Electric Vehicle. *SAE Int. J. Altern. Powertrains* **2012**, *1*, 134–143. [CrossRef]
16. Tan, S.; Yang, J.; Zhao, X.; Hai, T.; Zhang, W. Gear ratio optimization of a multi-speed transmission for electric dump truck operating on the structure route. *Energies* **2018**, *11*, 1324. [CrossRef]
17. Han, K.; Wang, Y.; Filev, D.; Dai, E.; Kolmanovsky, I.; Girard, A. Optimized design of multi-speed transmissions for battery electric vehicles. In Proceedings of the 2019 American Control Conference (ACC), Philadelphia, PA, USA, 10–12 July 2019; IEEE: Piscataway, NJ, USA, 2019; pp. 816–821. [CrossRef]
18. Li, Y.; Zhu, B.; Zhang, N.; Peng, H.; Chen, Y. Parameters optimization of two-speed powertrain of electric vehicle based on genetic algorithm. *Adv. Mech. Eng.* **2020**, *12*, 1687814020901652. [CrossRef]
19. Lucente, G.; Montanari, M.; Rossi, C. Modelling of an Automated Manual Transmission System. *Mechatronics* **2007**, *17*, 73–91. [CrossRef]
20. Mahmoudi, A.; Soong, W.L.; Pellegrino, G.; Armando, E. Efficiency maps of electrical machines. In Proceedings of the 2015 IEEE Energy Conversion Congress and Exposition (ECCE), Montreal, QC, Canada, 20–24 September 2015; pp. 2791–2799. [CrossRef]

21. Ehsani, M.; Gao, Y.; Gay, S. Characterization of electric motor drives for traction applications. In Proceedings of the 29th Annual Conference of the IEEE Industrial Electronics Society (IEEE Cat. No.03CH37468), Roanoke, NC, USA, 2–6 November 2003; pp. 891–896. [CrossRef]
22. Rahman, Z.; Ehsani, M.; Butler, K. An Investigation of Electric Motor Drive Characteristics for EV and HEV Propulsion Systems. In Proceedings of the Future Transportation Technology Conference & Exposition, Costa Mesa, CA, USA, 21–23 August 2000. [CrossRef]
23. Ehsani, M.; Rahman, K.M.; Toliyat, H.A. Propulsion system design of electric and hybrid vehicles. *IEEE Trans. Ind. Electron.* **1997**, *44*, 19–27. [CrossRef]
24. Raga, C.; Lázaro, A.; Barrado, A.; Martín-Lozano, A.; Quesada, I. Step-by-Step Small-Signal Modeling and Control of a Light Hybrid Electric Vehicle Propulsion System. *Energies* **2019**, *12*, 4082. [CrossRef]
25. Makrygiorgou, J.J.; Alexandridis, A.T. Power electronic control design for stable EV motor and battery operation during a route. *Energies* **2019**, *12*, 1990. [CrossRef]
26. Loncarski, J.; Leijon, M.; Srndovic, M.; Rossi, C.; Grandi, G. Comparison of output current ripple in single and dual three-phase inverters for electric vehicle motor drives. *Energies* **2015**, *8*, 3832–3848. [CrossRef]
27. Shi, Y.; Wei, J.; Deng, Z.; Jian, L. A Novel Electric Vehicle Powertrain System Supporting Multi-Path Power Flows: Its Architecture, Parameter Determination and System Simulation. *Energies* **2017**, *10*, 216. [CrossRef]
28. Zhu, B.; Zhang, N.; Walker, P.; Zhan, W.; Yueyuan, W.; Ke, N.; Zhou, X. Two motor two speed power-train system research of pure electric vehicle. In Proceedings of the SAE 2013 World Congress & Exhibition, Detroit, MI, USA, 16–18 April 2013. [CrossRef]
29. Kim, H.; Wi, J.; Yoo, J.; Son, H.; Park, C.; Kim, H. A study on the fuel economy potential of parallel and power split type hybrid electric vehicles. *Energies* **2018**, *11*, 2103. [CrossRef]
30. Roozegar, M.; Setiawan, Y.; Angeles, J. Design, modelling and estimation of a novel modular multi-speed transmission system for electric vehicles. *Mechatronics* **2017**, *45*, 119–129. [CrossRef]
31. Roozegar, M.; Angeles, J. The optimal gear-shifting for a multi-speed transmission system for electric vehicles. *Mech. Mach. Theory* **2017**, *116*, 1–13. [CrossRef]
32. Han, P.; Cheng, X.S.; Huang, Y.; Gu, Q.; Hu, H.B. Research on the shift schedule of dual clutch transmission for pure electric vehicle. *Appl. Mech. Mater.* **2014**, *496–500*, 1318–1321. [CrossRef]
33. Zhu, B.; Zhang, N.; Walker, P.; Zhan, W.Z.; Zhou, X.X.; Ruan, J.G. Two-Speed DCT Electric Powertrain Shifting Control and Rig Testing. *Adv. Mech. Eng.* **2013**, *5*, 323917. [CrossRef]
34. Liang, Q.; Tang, N.; Gao, B.; Chen, H. The seamless gear shifting control for pure electric vehicle with 2-speed inverse-AMT. *IFAC Proc. Vol.* **2013**, *46*, 507–511. [CrossRef]
35. Fang, S.N.; Song, J.; Song, H.J.; Tai, Y.Z.; Li, F.; Nguyen, T.S. Design and control of a novel two-speed Uninterrupted Mechanical Transmission for electric vehicles. *Mech. Syst. Signal. Process.* **2016**, *75*, 473–493. [CrossRef]
36. Chai, B.; Zhang, J.; Wu, S. Compound optimal control for shift processes of a two-speed automatic mechanical transmission in electric vehicles. *Proc. Inst. Mech. Eng. Part. D Int. J. Automot. Mech. Eng.* **2019**, *233*, 2213–2231. [CrossRef]
37. Kim, Y.-K.; Kim, H.-W.; Lee, I.-S.; Park, S.-M.; Mok, H.-S. A speed control for the reduction of the shift shocks in electric vehicles with a two-speed AMT. *J. Power Electron.* **2016**, *16*, 1355–1366. [CrossRef]
38. Zhou, X.; Walker, P.; Zhang, N.; Zhu, B.; Ruan, J. Numerical and experimental investigation of drag torque in a two-speed dual clutch transmission. *Mech. Mach. Theory* **2014**, *79*, 46–63. [CrossRef]
39. Kidambi, N.; Harne, R.; Fujii, Y.; Pietron, G.M.; Wang, K. Methods in vehicle mass and road grade estimation. *SAE Int. J. Passeng. Cars Mech. Syst.* **2014**, *7*, 981–991. [CrossRef]
40. Jauch, J.; Masino, J.; Staiger, T.; Gauterin, F. Road grade estimation with vehicle-based inertial measurement unit and orientation filter. *IEEE Sens. J.* **2018**, *18*, 781–789. [CrossRef]
41. Jo, K.; Lee, M.; Sunwoo, M. Road slope aided vehicle position estimation system based on sensor fusion of GPS and automotive onboard sensors. *IEEE Trans. Intell. Transp. Syst.* **2015**, *17*, 250–263. [CrossRef]
42. Karoshi, P.; Ager, M.; Schabauer, M.; Lex, C. Robust and numerically efficient estimation of vehicle mass and road grade. In *Advanced Microsystems for Automotive Applications 2017*; Zachäus, C., Müller, B., Meyer, G., Eds.; Springer: Cham, Switzerland, 2018; pp. 87–100. [CrossRef]
43. Kim, S.; Shin, K.; Yoo, C.; Huh, K. Development of algorithms for commercial vehicle mass and road grade estimation. *Int. J. Automot. Technol.* **2017**, *18*, 1077–1083. [CrossRef]

44. Liao, X.; Huang, Q.; Sun, D.; Liu, W.; Han, W. Real-time road slope estimation based on adaptive extended Kalman filter algorithm with in-vehicle data. In Proceedings of the 2017 29th Chinese Control and Decision Conference (CCDC), Chongqing, China, 28–30 May 2017; pp. 6889–6894. [CrossRef]
45. Kidambi, N.; Pietron, G.M.; Boesch, M.; Fujii, Y.; Wang, K.-W. Accuracy and robustness of parallel vehicle mass and road grade estimation. *SAE Int. J. Veh. Dyn. Stab. NVH* **2017**, *1*, 317–325. [CrossRef]
46. Zhang, Z.; Zuo, C.; Hao, W.; Zuo, Y.; Zhao, X.; Zhang, M. Three-speed transmission system for purely electric vehicles. *Int. J. Automot. Technol.* **2013**, *14*, 773–778. [CrossRef]
47. Shen, W.; Yu, H.; Hu, Y.; Xi, J. Optimization of shift schedule for hybrid electric vehicle with automated manual transmission. *Energies* **2016**, *9*, 220. [CrossRef]
48. Xiang, Y.; Guo, L.; Gao, B.; Chen, H. A study on gear shifting schedule for 2-speed electric vehicle using dynamic programming. In Proceedings of the 2013 25th Chinese Control and Decision Conference (CCDC), Guiyang, China, 25–27 May 2013; pp. 3805–3809. [CrossRef]
49. Lin, C.; Zhao, M.; Pan, H.; Yi, J. Blending gear shift strategy design and comparison study for a battery electric city bus with AMT. *Energy* **2019**, *185*, 1–14. [CrossRef]
50. Amari, S.I. Backpropagation and stochastic gradient descent method. *Neurocomputing* **1993**, *5*, 185–196. [CrossRef]
51. Momma, M.; Bennett, K.P. A pattern search method for model selection of support vector regression. In Proceedings of the 2002 SIAM International Conference on Data Mining, Arlington, VA, USA, 11–13 April 2002; pp. 261–274. [CrossRef]